SAND79-2043
Unlimited Release

UC-13

ACOUSTICAL STUDIES OF BOILING INSTABILITIES IN THE PROTOTYPE RECEIVER FOR THE BARSTOW SOLAR PILOT PLANT

Alan G. Beattie

Prepared by Sandia Laboratories, Albuquerque, New Mexico 87185 and Livermore, California 94550 for the United States Department of Energy under Contract AT(29-1)-789

Printed November 1979

Sandia Laboratories

Issued by Sandia Laboratories, operated for the United States Department of Energy by Sandia Corporation.

NOTICE

Printed in the United States of America

Available from
National Technical Information Service
U. S. Department of Commerce
5285 Port Royal Road
Springfield, VA 22161

Price: Printed Copy **$4.50** ; Microfiche $3.00

SAND79-2043
Unlimited Release
Printed November 1979

UC-13

ACOUSTICAL STUDIES OF BOILING INSTABILITIES IN THE PROTOTYPE RECEIVER FOR THE BARSTOW SOLAR PILOT PLANT

Alan G. Beattie
Nondestructive Testing Technology Division 1552
Sandia Laboratories
Albuquerque, New Mexico 87185

ABSTRACT

An acoustic technique is used to search for proposed boiling instabilities in the prototype receiver for the Barstow 10 MW Solar Thermal Pilot Plant. The technique is shown to work and should be capable of measuring such instabilities when the receiver is tested at maximum proposed power levels.

ACKNOWLEDGMENT

This experiment was made possible by the enthusiastic cooperation of the following two companies: Acoustic Emission Technology, who modified and reprogrammed their source location system for lease and then cheerfully put up with an incredible number of schedule changes; and Dunegan/Endevco, who designed and built the acoustic emission transducers specifically for this experiment and did it in record time. Much of the supervisison and work in the daily running of the data acquisition system was ably carried out by Jean Kinker, Division 1552.

LIST OF FIGURES

LIST OF FIGURES
(continued)

ACOUSTICAL STUDIES OF BOILING INSTABILITIES IN THE PROTOTYPE RECEIVER FOR THE BARSTOW SOLAR PILOT PLANT

Introduction

A theoretical study of the receiver design for the Barstow 10 MW Solar Thermal Pilot Plant raised the possibility of a boiling instability during steady state operation. This instability would be an oscillatory movement of the transition region between nucleate and film boiling. The period of this oscillation of the departure from nucleate boiling (DNB) zone was predicted to be around three seconds with an unknown amplitude. If such an oscillation exists with a large amplitude, it could have a serious effect on the life span of the receiver. The differences in thermal conductivity between a metal surface wet with a film of water and one with a vapor film between it and the water could lead to a surface temperature 100°F hotter in the film boiling region. Thermal fatigue could rapidly occur if a region of the receiver experienced such fluctuations at more than 10^4 cycles per operating day.

The prototype receiver is well instrumented with thermocouples on the outside surface of the tube. However, thermal inertia of the metal tubes will prevent their outside surface from responding to thermal oscillations inside the tubes of this frequency. A natural reluctance to breach the integrity of the tubes to put thermocouples on the interior wall led to this attempt to determine the position and stability of the DNB zone using acoustic techniques.

The acoustic approach is based on two simple premises. First, nucleate boiling produces many acoustic signals. Preliminary investigation indicated

a high level of acoustic energy with frequency components up to 400 kHz. Second, the transfer of acoustic energy across an interface between metal and water is much greater when the water wets the surface than when a film of vapor separates the water from the metal. The preliminary investigation also suggested that this premise is correct. A computer model of the proposed experiment was designed. When the model indicated that the experiment appeared feasible, the decision was made to attempt to locate the DNB zone acoustically.

This progress report gives the results of the attempt to use acoustic techniques to locate the DNB zone. All work reported here was done during the low power phase of the testing of the prototype receiver. The main purpose of the experiments at this power level was not to search for instabilities but to develop and prove the acoustic technique.

The actual location of the position of the DNB zone in the receiver appears to be somewhat model dependent. Depending upon the mathematical details, there can be a variation of up to a meter in the location of the base line position of the zone. However, the amplitudes and frequency of the fluctuations around the base line appear almost totally independent of the fine structure of the model. At present, this acoustic technique appears to give a general location to the DNB zone and measures the fluctuations around this location with high accuracy. Thus the technique appears successful and gives us confidence that any instabilities in the DNB zone which occur during the high power tests will be identified and measured.

Mathematical Approach

The receiver, which consists of 70 parallel 1/2-inch O.D. incoloy tubes welded together into a plate, is treated mathematically as a two-dimensional anisotropic plate. It is assumed that acoustic energy is generated in the region where nucleate boiling occurs. This energy is composed of many individual acoustic bursts with the average time between bursts much shorter than the decay time of the bursts. Thus the character of the signal is that of a "white" noise signal with a high frequency cut off. It is assumed here that the only important characteristic of this signal, within a fixed frequency range, is its amplitude. It is further assumed that enough bursts are present so that random fluctuations in the signal amplitude over the sampling time - $\sim$ 100 μseconds - are small and this allows the determination of an acoustic generation profile over the surface of the plate. Because the diameter of the focus of the solar beams is wider than the horizontal dimension of the receiver, the acoustic generation profile is assumed to be constant across the receiver. The acoustic amplitude at any position on the receiver can then be written as

$$A_i^2 = A_o^2 \int_{-a}^{+a} \int_{o}^{C} (Y) e^{-2(\alpha^2 (x-W_i)^2 + \beta^2 (y-V_i)^2)^{\frac{1}{2}}} \, dy dx \qquad (1)$$

where A_i is the acoustic amplitude at point i, A_o is the maximum acoustic amplitude, a is the horizontal half width of the receiver where the center of the plate is zero, C, the position of the DNB zone with the bottom of the receiver at zero, Y is the vertical acoustic generation function,

α and β are the horizontal and vertical acoustic attenuations, and W_i and V_i are the horizontal and vertical coordinates of the point.

Critical to the use of this equation is the determination of the acoustic generation function, Y. After several attempts, a function was found which gave a reasonable fit to the experimental data. This function is

$$Y = \tfrac{1}{2}(1 + \tanh(r(y - C/s))) \tag{2}$$

where r and s are constants obtained by making a best fit to a data set. Since the integration along y is taken only to the point C, we are setting Y = 0 for all y between C and the top of the receiver. The range of values for r is limited to $0.1 \leq r \leq 5.0$ and for s, $1.5 \leq s \leq 8.0$. Figure 1 gives Y for C = 10.0, r = 2.0 and s = 8.0. Figure 2 gives Y for C = 10.0, r = 0.2 and s = 2.0. Large values of r correspond physically to an onset of nucleate boiling at a very localized elevation on the receiver while large values of s correspond to nucleate boiling extending a long distance along the receiver before the DNB zone is reached.

Equation (1) then has only two unknowns, C and A_o, if we assume that r and s are fixed for a day's experimental run. By sampling the acoustic amplitude at several points we can obtain a set of equations in two unknowns. The main problem arises from the fact that Equation (1) is not analytically integrable for most functions, Y. The approach used here is to sample the acoustic amplitudes at a large number of points (20 in this experiment) and then use a non-linear least squares program on a large computer to solve this set of equations for C and A_o. This solution involves many numerical integrations but can be done in a somewhat reasonable time ($\sim$ 1/2 second) on a CDC 7600.

Experimental Details

To insure that the set of equations were overdetermined and that there was adequate coverage over the length of the receiver, 20 transducers were used. These were arranged on the receiver in the pattern shown in Figure 3. The array was intended to be symmetrical but various obstructions on the back of the receiver resulted in the pattern shown. The outer transducers, five each, are mounted on tubes #5 and #66 while the center ten transducers are mounted on tube #34.

The transducers are Dunegan/Endevco S9205M4 transducers which were developed specifically for this installation. They are designed to function up to 1200°F and to date have survived excursions up to 1360°F. They are mounted as shown in Figure 4 to studs welded to the receiver tubes. The couplant used between the transducer and the stud is a mixture of 50% In and 50% Ga. Stainless steel coaxial cables, integral with the transducer, bring the signals out of the high temperature region where a connection is made to RG 196 coaxial cable with microdot connectors. With this layout, there are no soldered connections until the 10 ft long cable reaches the preamplifier. The preamplifiers are mounted in the receiver support tower and are connected to the data acquisition system with 100 ft power-signal cables.

Acoustic Emission Technology (AET) 140A preamplifiers are used with a 125-250 kHz band pass filter. The data acquisition system is a leased AET source location system. This system can sample the RMS voltage from all twenty transducers up to 100 times per second and write this information digitally on a 9-track magnetic tape. To date, all data has been taken at a sampling rate of 10 data sets per second. The overall system

gain is set at 94 dB. At this setting the preamplifier noise level will register 0 or 1 RMS voltage unit and the normal signal levels range between 30 and 500 voltage units. The digital system saturates at 1024 voltage units.

Data for all runs was taken for a period of approximately 300 seconds after the receiver had reached an equilibrium for that test point. The condition of equilibrium was determined by receiver operating personnel who would then notify our operator and give the test point designation. All data was stored digitally on magnetic tape and kept for future analysis.

Data Processing

The original test plan was to take calibration data for the transducers by introducing a white noise signal into one transducer and measuring the output of the other 19 transducers. This will give 400 equations in 23 unknowns, the 20 coupling coefficients, the x and y acoustic attenuations and the signal amplitude. Preamplifier gains were included in the calibration. This calibration procedure was tried but the resulting coupling coefficients did not give reasonable results when used with actual data. The problem appears to be that the transducers, with this mounting method, do not appear to be reciprocal devices; i.e., the efficiencies for generating and receiving acoustic waves are not the same. While there are an adequate number of equations to solve for the 43 unknowns necessary to account for different generating and receiving efficiencies, the existing nonlinear least squares program could not handle that many unknowns without nontrivial modifications. The combinations of a limited time available and the probability that small changes in the coupling coefficients and/or transducer efficiencies will occur between

runs, made this approach seem not worth pursuing at present. The only numbers used from the calibration were the attenuation coefficients. These were, for the receiver filled with 200°F water, $\alpha = 2.0\ m^{-1}$ and $\beta = 0.27\ m^{-1}$. While the attenuation coefficients showed some variation between different measurements under different conditions and by different methods, α was always an order of magnitude greater than β.

The problems of day-to-day changes in coupling efficiencies and preamplifier gains and the problem that the acoustic generation function is only an approximation were solved in the following way. It was assumed that the gains and transducer efficiencies would not change during a day's run. With less justification it was also assumed that the acoustic generation function would be essentially constant over the test conditions investigated during one day. With these assumptions, effective coupling coefficients were determined for one day's run. These coefficients contain the preamplifier gain, the transducer coupling coefficient and the effect of the deviation between the actual and the assumed acoustic generation function. To obtain these coefficients, ten consecutive sets of typical data were taken from each test point on that day. These were averaged within each test point and one averaged set was used to find the best acoustic generation function. This was done by varying the parameters r and s until the best fit to the data was obtained (the non-linear least squares program gives a measure of the goodness of fit). These values for r and s were then used with all the averaged data sets. C and A_o were calculated for each data set. These values were then used in Equation (1) to calculate the expected noise amplitude at each transducer. The effective coupling coefficient, K_i, for each transducer is then given by

$$K_i = A_i(\text{averaged})/A_i(\text{calculated}). \tag{3}$$

This was done for each averaged data set and the K_i from each transducer were then averaged over all the test points taken during that day. The averaged K_i along with the values for r and s were used to analyze all the data taken during that day. The set of equations solved for each data set are then

$$A_i^2 = \frac{1}{2} A_o^2 K_i^2 \int_{-a}^{+a} \int_{o}^{C} (1 + \tan h\ (r(y - \tfrac{C}{s})))e^{-2(\alpha^2(x-W_i)^2 + \beta^2(y-V_i)^2)^{\frac{1}{2}}} dy\ dx. \tag{4}$$

This set of equations was solved for the first 2,500 data sets recorded for each test point.

The 2,500 solutions per test point were graphed as a function of time. In order to make the data more intelligible, several smoothing procedures were used. First, any solution point greater than 12.5 meters, which is the top of the receiver, was set equal to 12.5. Then any solution point which varied by more than ±3% from the average of itself and the previous four points was replaced by (1 ±.03) times this average. This procedure removed random points which did not follow a trend but had little effect on the overall curves. Finally, the points were smoothed by averaging the data point with the four points which preceded it and the four points which followed it in time. This smoothing procedure is effectively a low pass filter which damps fluctuations with frequencies above about 2 Hz. Many checks were run comparing these

smoothed curves against curves of the unsmoothed solutions to insure that only "noise" was being removed and not any significant features. The graphs for the test points analyzed to date are shown in Figures 5 through 19.

Accuracy of the Analysis

The following questions must be raised because of the complexity and empirical nature of the mathematical analysis. First, do these curves have any relationship with the position of the DNB zone and if so, what is it? Second, what is the effect of small changes in the mathematical parameters, such as the acoustic generation function constants, the transducer effective coupling constants and the acoustic attenuations? The first question is answered by test point 3.2A, shown in Figure 6. During this test point, a cloud passed over the mirror field. The resulting loss in power caused wet steam to pass from the receiver into the down comer line, indicating that the DNB zone had reached the top of the receiver. This is exactly what is shown in Figure 6 and is strong evidence that the acoustic measurements are indicating the position of the DNB zone.

The effect of changing the constants in the acoustic generation function was explored on test point 21.09. An expanded plot of part of this test point is shown in Figure 20. In this calculation, the acoustic generation function shown in Figure 1 was used. The curve was then recalculated using the acoustic generation function shown in Figure 2, along with the corresponding changes in the transducer coupling constants. The curve corresponding to Figure 20 is plotted in Figure 21. The net effect of using two quite different acoustic generation functions was to

shift the base line positions by about 0.8 meters. However, a close comparison of Figures 20 and 21 will show little difference in even the finest detail between the two curves. The conclusion to be drawn from this example is that while the use of different fitting parameters may effect the position of the base line of the DNB zone position curve, the fine structure of the curve, including the amplitude and frequency of the excursions, is almost independent of the values of the fitting parameters.

Independent Oscillations in the Tubes

It has been suggested that besides the possibility of the DNB zone moving coherently up and down the receiver, each individual tube may contain an oscillation, independent of all the other tubes. The acoustic data is derived from acoustic signals generated in all parts of the receiver. However, the transducers are mounted on three widely separated tubes. The relatively high attenuation coefficient in the x direction should give some decoupling of the acoustic signals between rows of transducers. Five transducers do not give enough equations to produce accurate locations, but the central 10 transducers should be capable of being analyzed by themselves. Again test 21.09 was used for this analysis. Data from only the 10 central transducers was used to produce Figure 22. Comparing with Figure 20, again a shift in the base line is seen but the fine structure is almost identical. These curves suggest that the DNB zone may have the shape of a curve instead of a horizontal line across the receiver but the movement of the zone is a coherent motion across the entire receiver.

Conclusion

The data analysis performed to date strongly indicates that this acoustic technique gives accurate information about variations in the

position of the DNB zone. There is a model dependence in the calculation that leads to an ambiguity of about a meter in the location of the time averaged position of the DNB zone. However, the amplitudes and fine structure of the excursions of the DNB zone from this average position appear model independent. Such excursions are the instability that this experiment was designed to measure. This technique appears fully capable of determining whether the position of the DNB zone is stable at high power levels. If the zone is not stable, the technique can measure the amplitudes and periods of the instabilities.

FIGURE 1
THE ACOUSTIC GENERATION FUNCTION FOR
C = 10.0, r = 2.0 AND s = 8.0

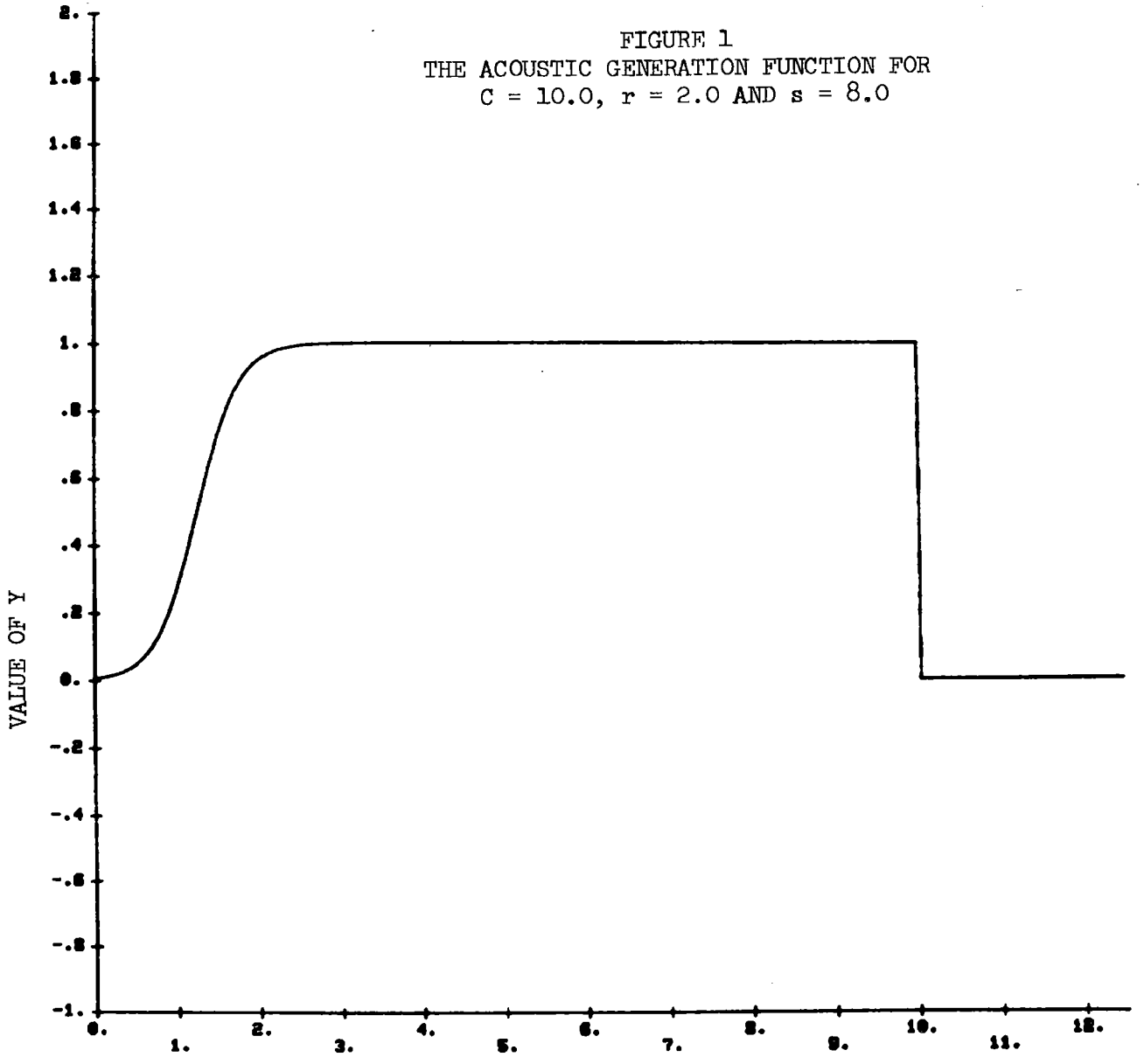

FIGURE 2
THE ACOUSTIC GENERATION FUNCTION FOR
C = 10.0, r = 0.2 AND s = 2.0

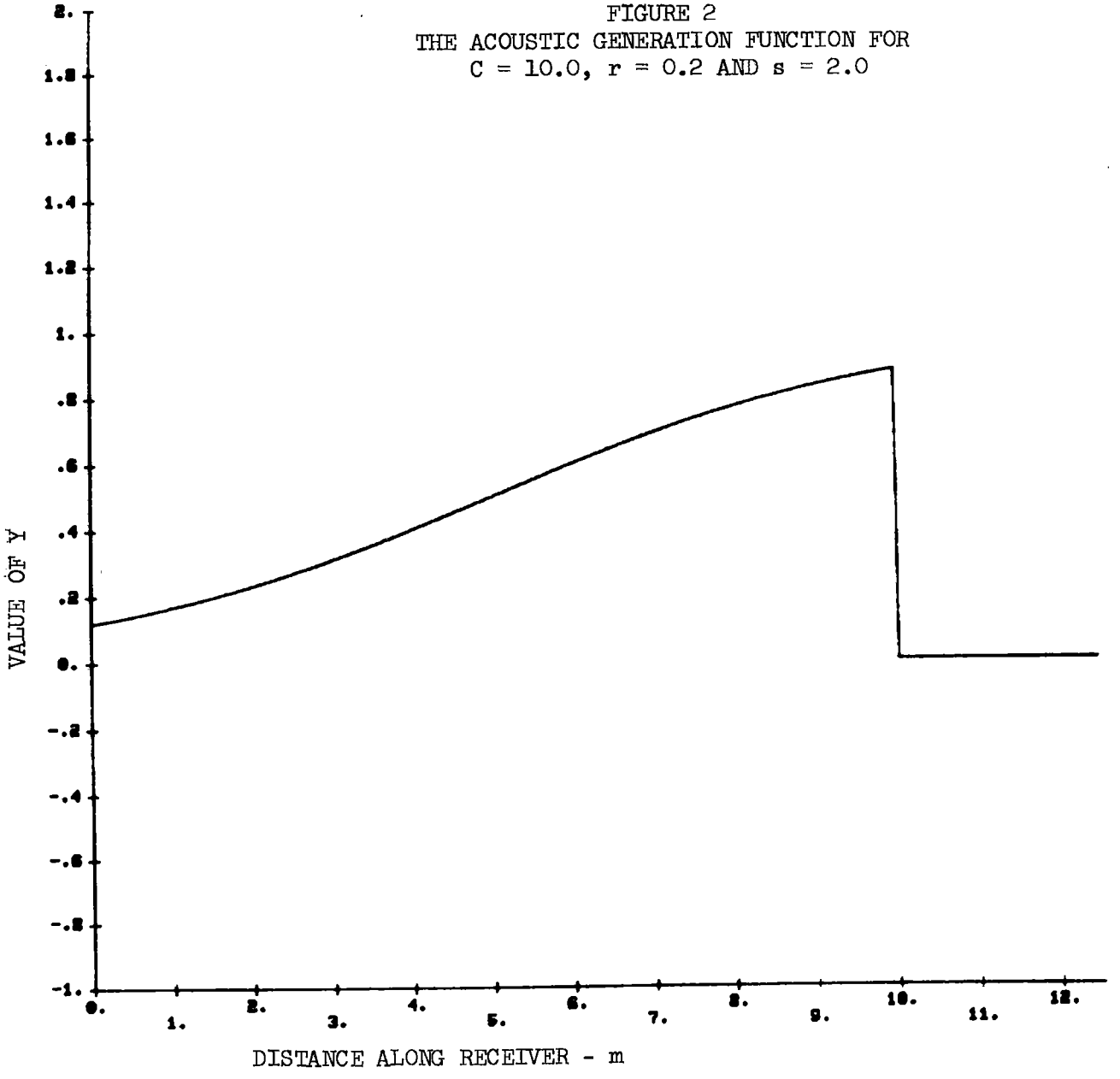

FIGURE 3
THE LAYOUT OF THE TRANSDUCER ARRAY ON THE RECEIVER. THE HORIZONTAL DIMENSION HAS BEEN MAGNIFIED FOR CLARITY.

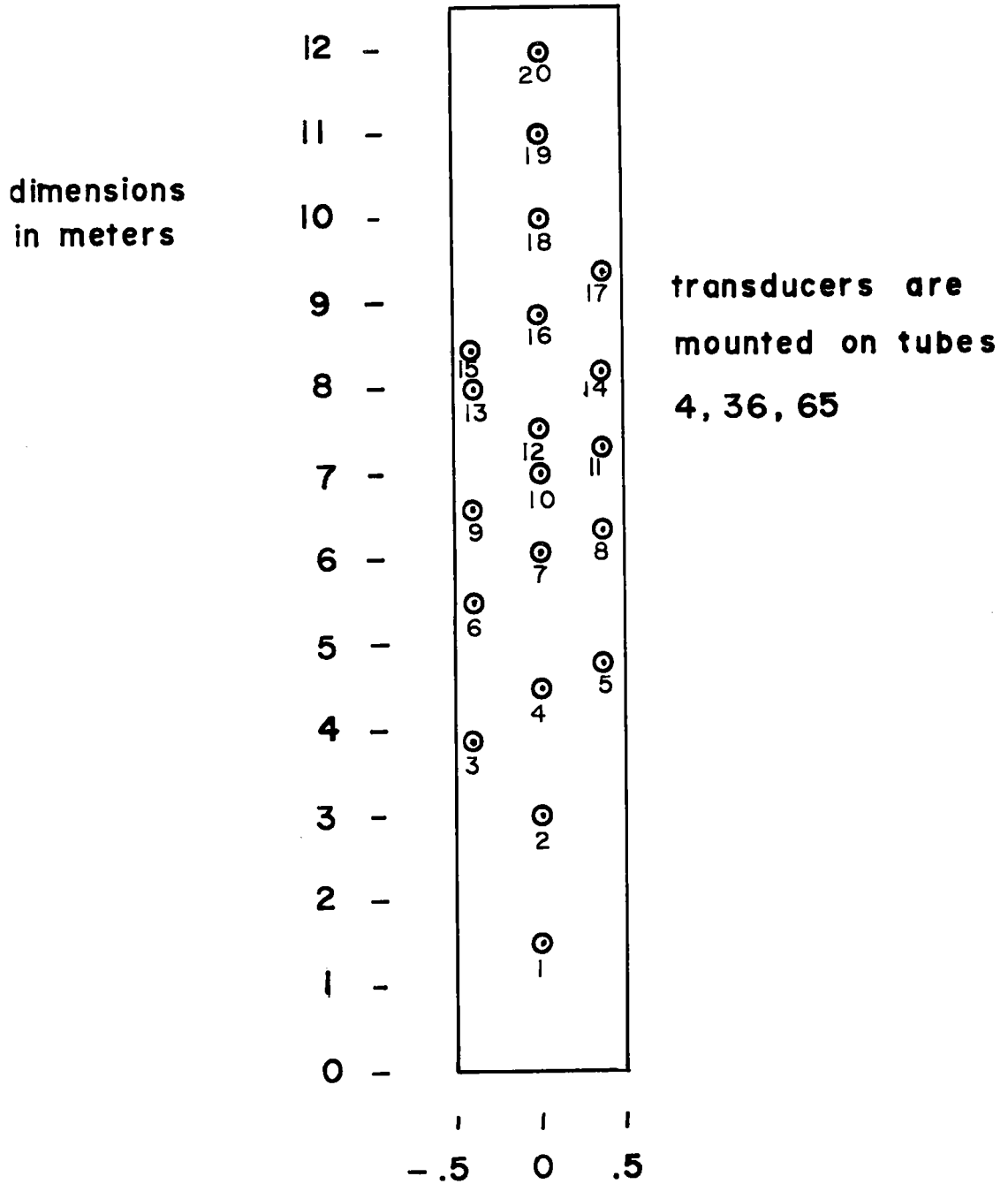

FIGURE 4
DIAGRAM OF TRANSDUCER AND MOUNTING STUD

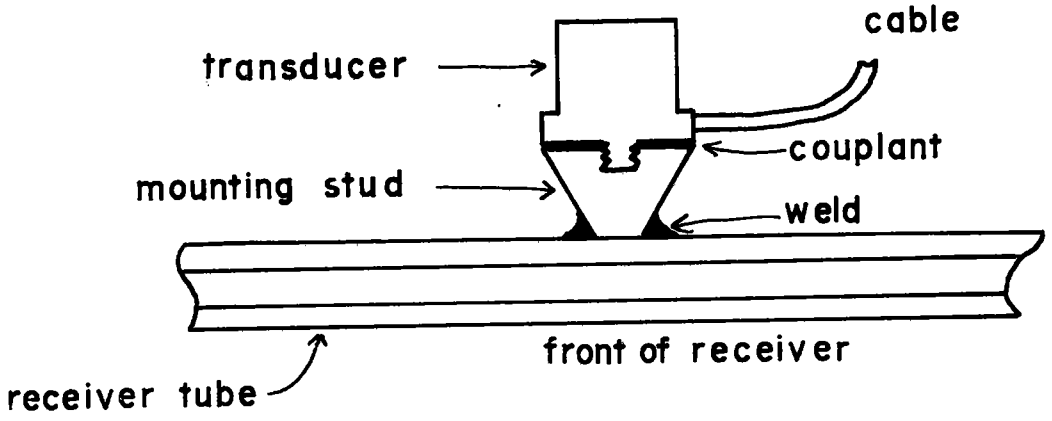

FIGURE 5
TEST POINT 3.1
8 MAY 1979
ZERO SECONDS STARTS AT 12:02:59 HOURS

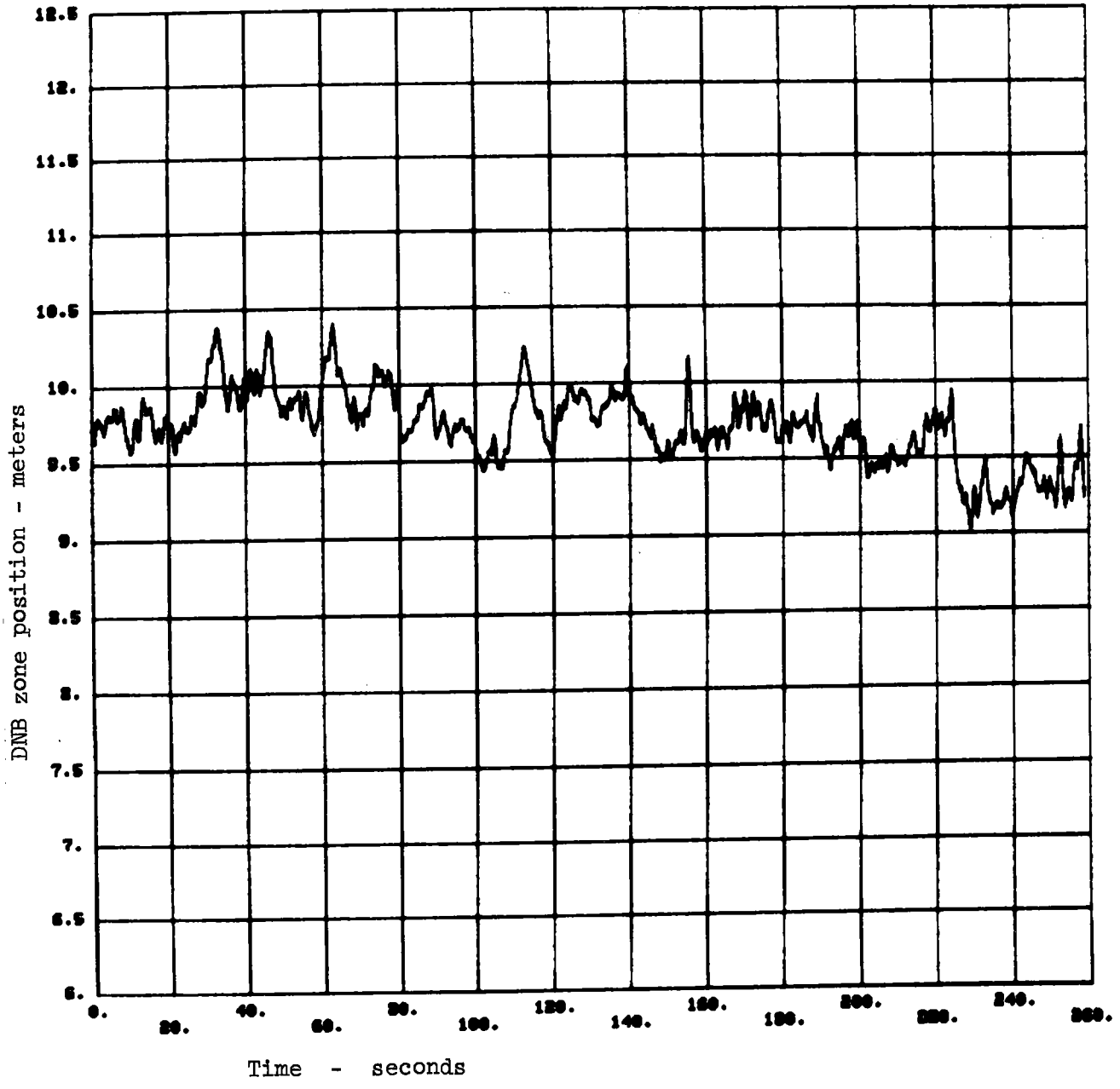

FIGURE 6
TEST POINT 3.2-A
8 MAY 1979
ZERO SECONDS STARTS AT 12:17:40 HOURS

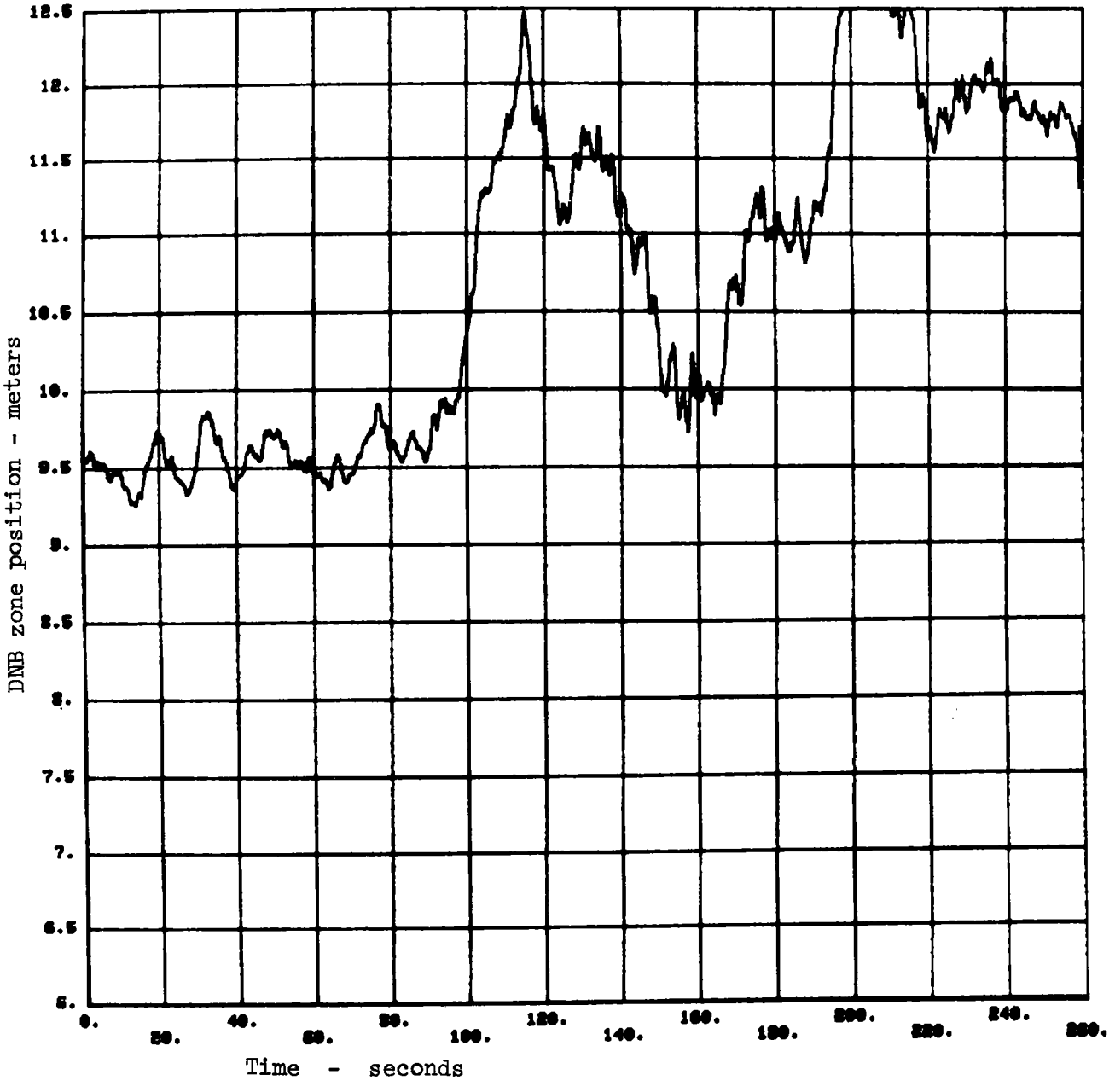

FIGURE 7
TEST POINT 3.2-B
8 MAY 1979
ZERO SECONDS STARTS AT 12:29:05 HOURS

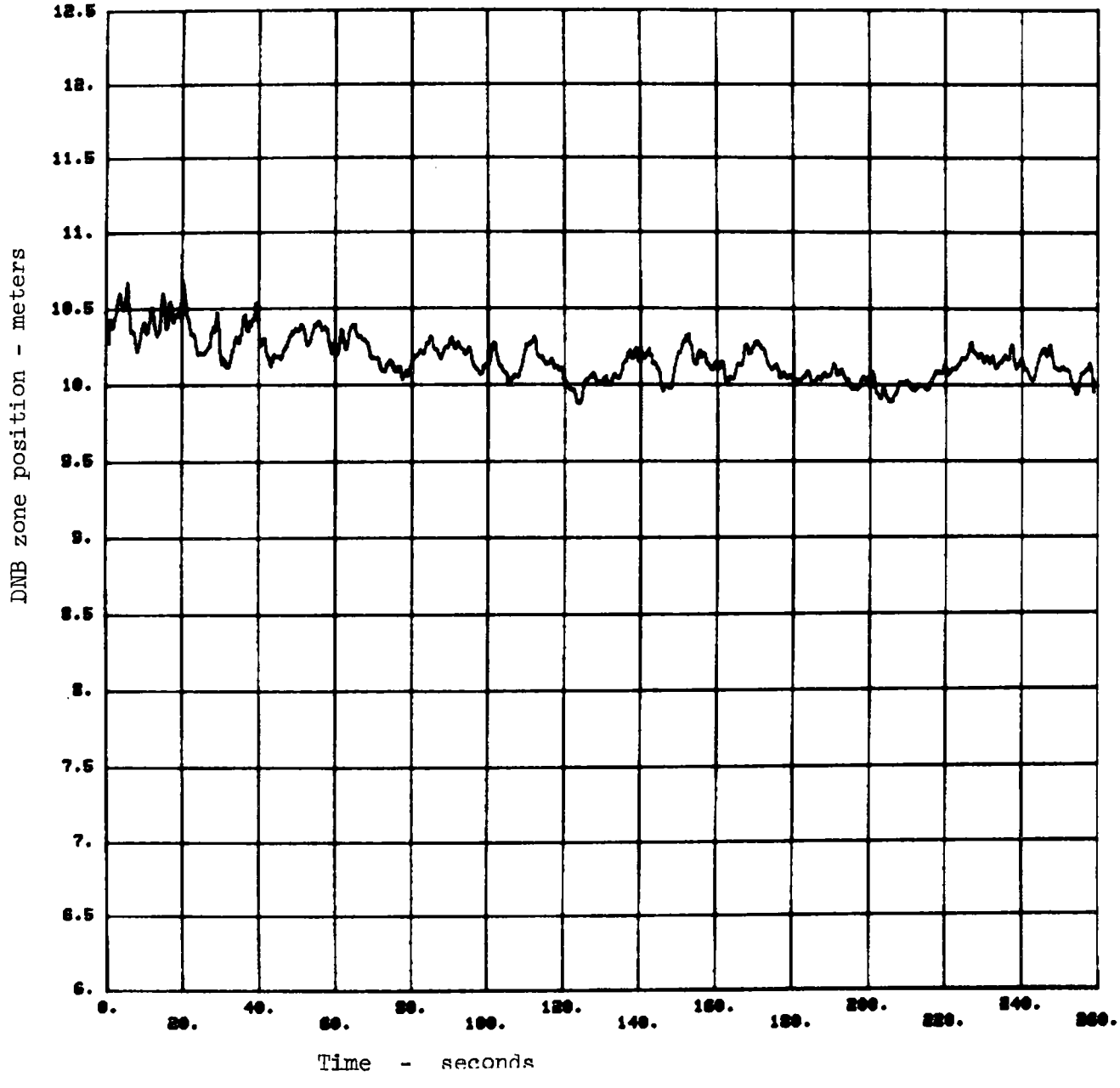

FIGURE 8
TEST POINT 3.3
8 MAY 1979
ZERO SECONDS STARTS AT 12:45:14 HOURS

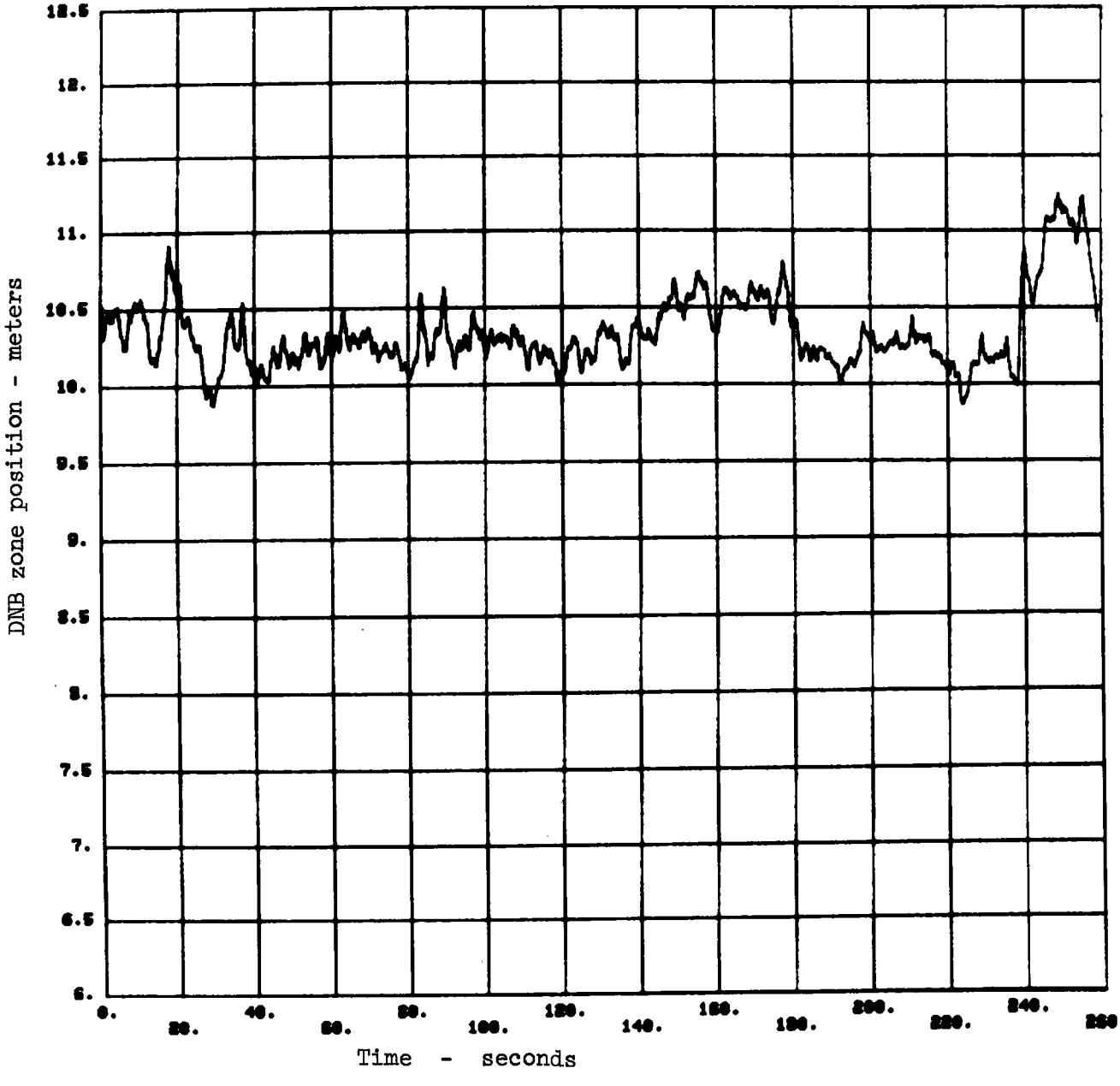

FIGURE 9
TEST POINT 3.4
8 MAY 1979
ZERO SECONDS STARTS AT 13:43:18 HOURS

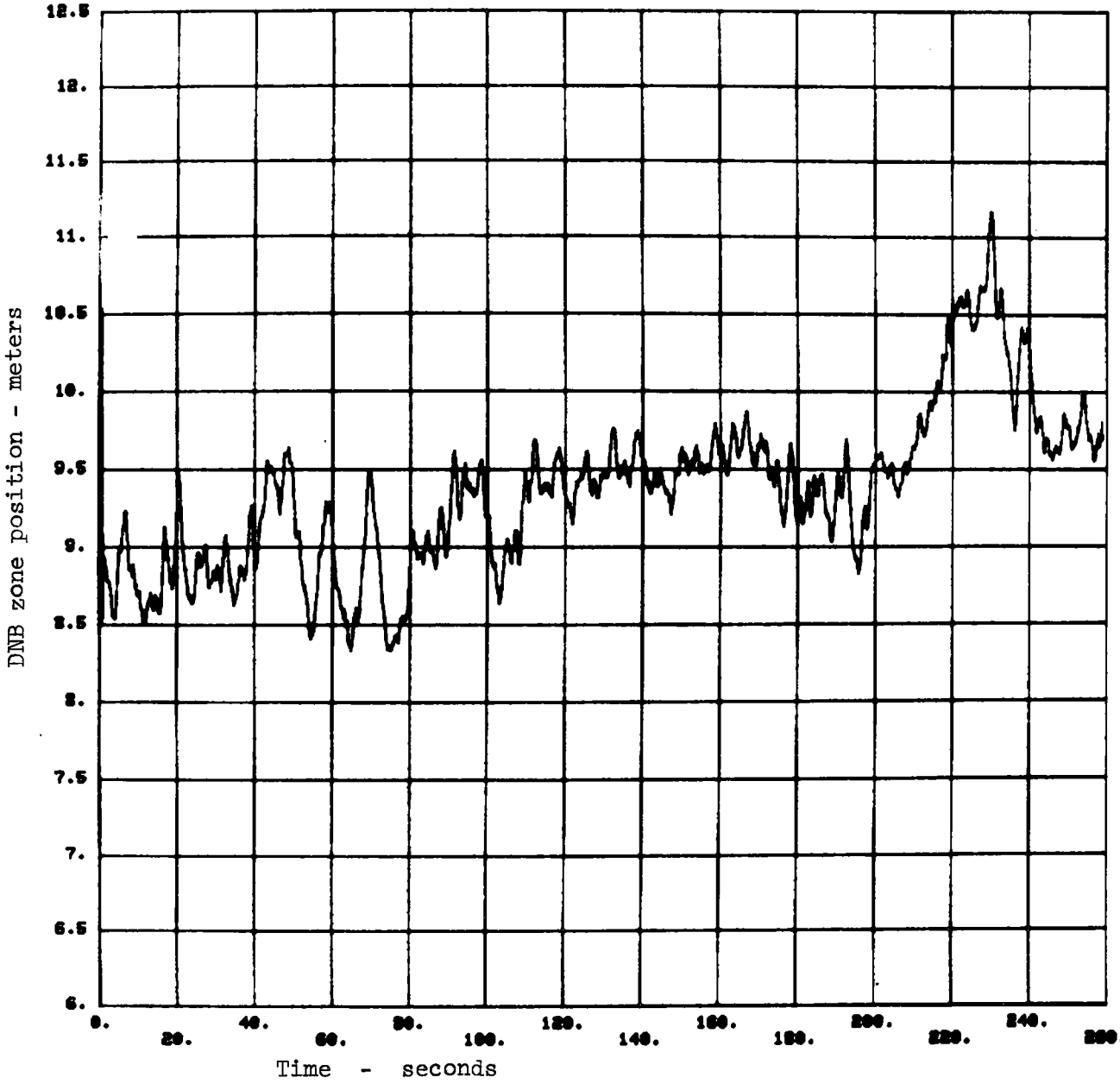

FIGURE 10
TEST POINT 5.1
13 JUNE 1979
ZERO SECONDS STARTS AT 11:04:18 HOURS

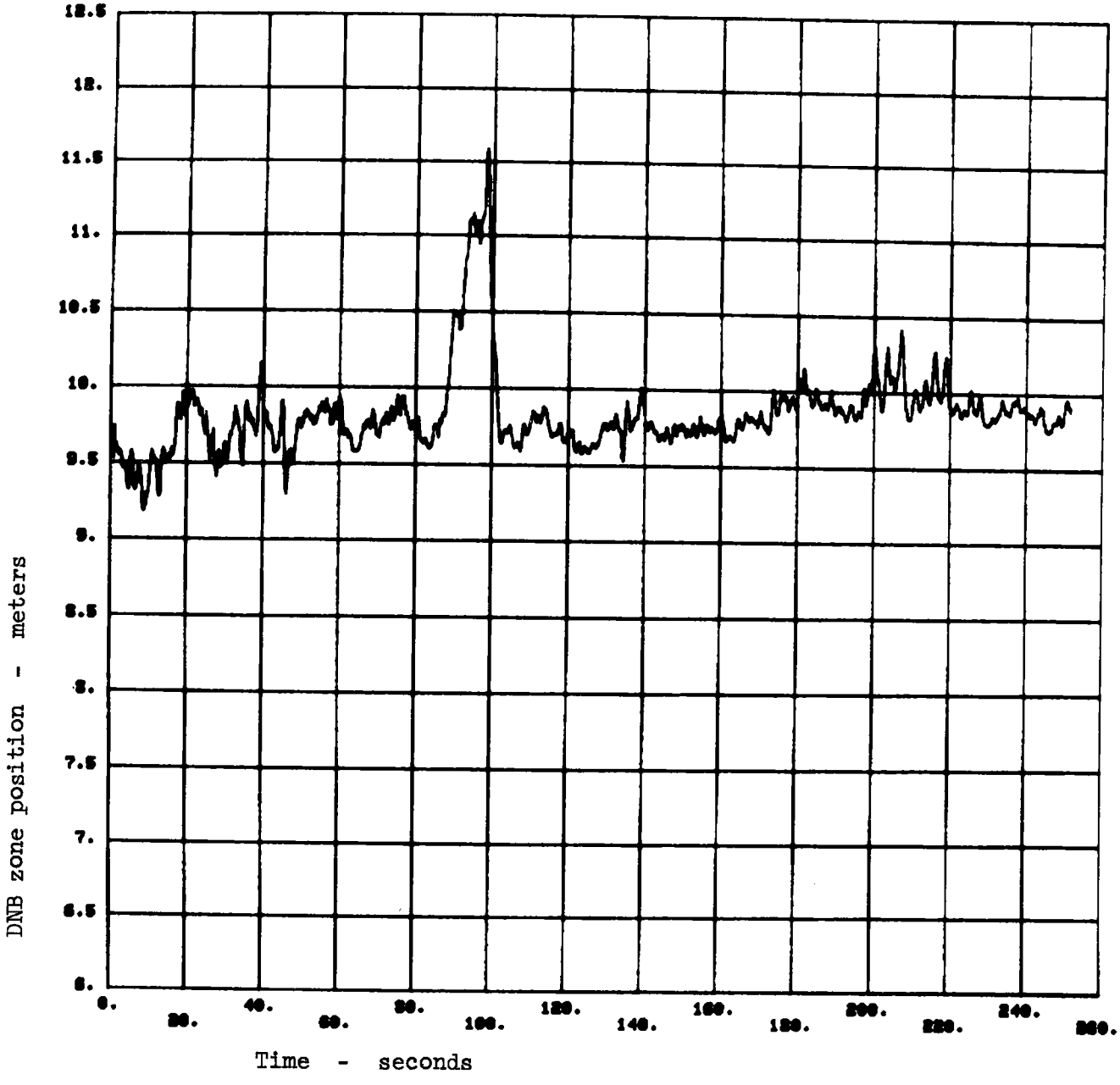

FIGURE 11
TEST POINT 5.2
13 JUNE 1979
ZERO SECONDS STARTS AT 12:50:50 HOURS

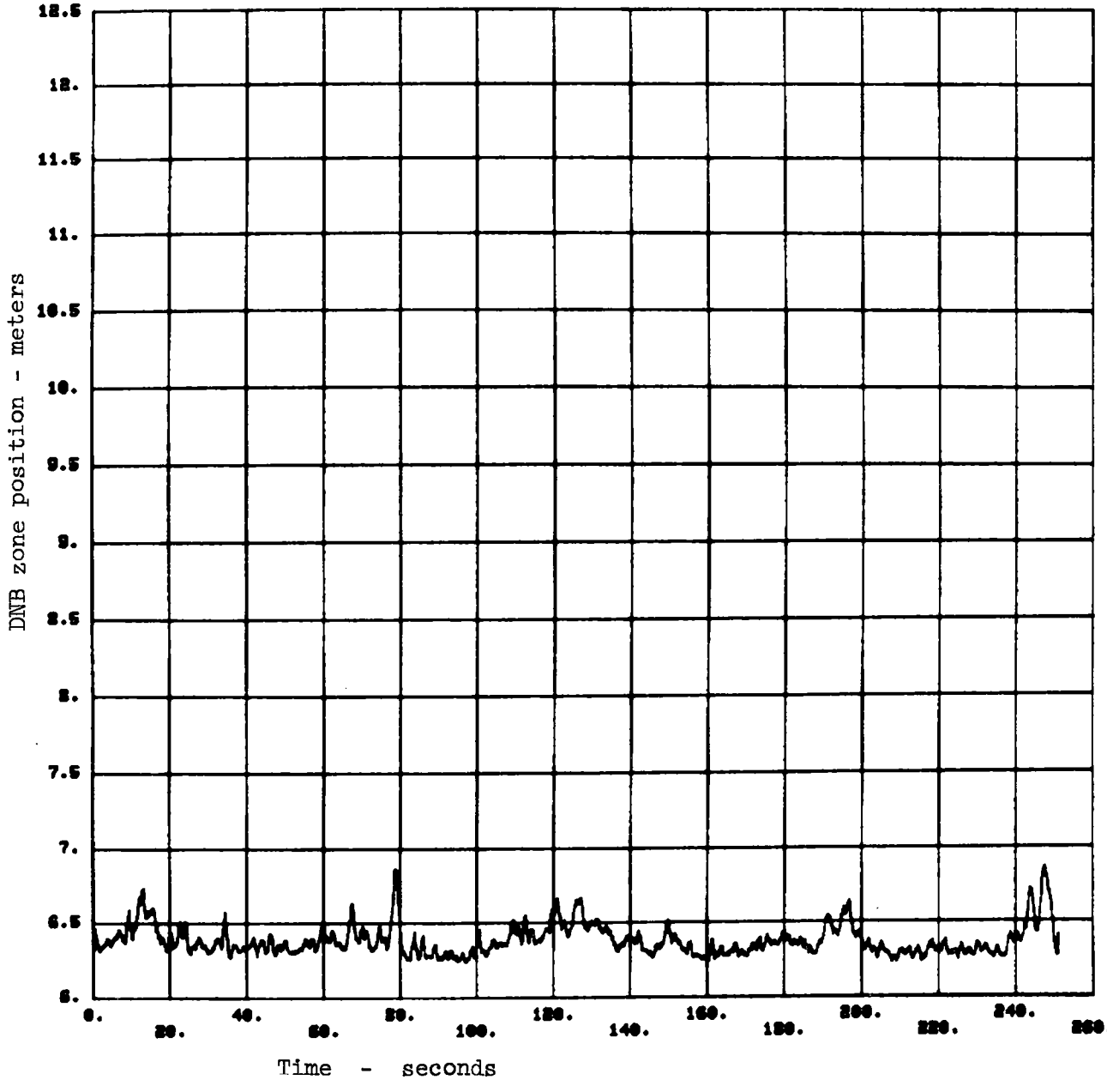

FIGURE 12
TEST POINT 5.3
13 JUNE 1979
ZERO SECONDS STARTS AT 14:06:04 HOURS

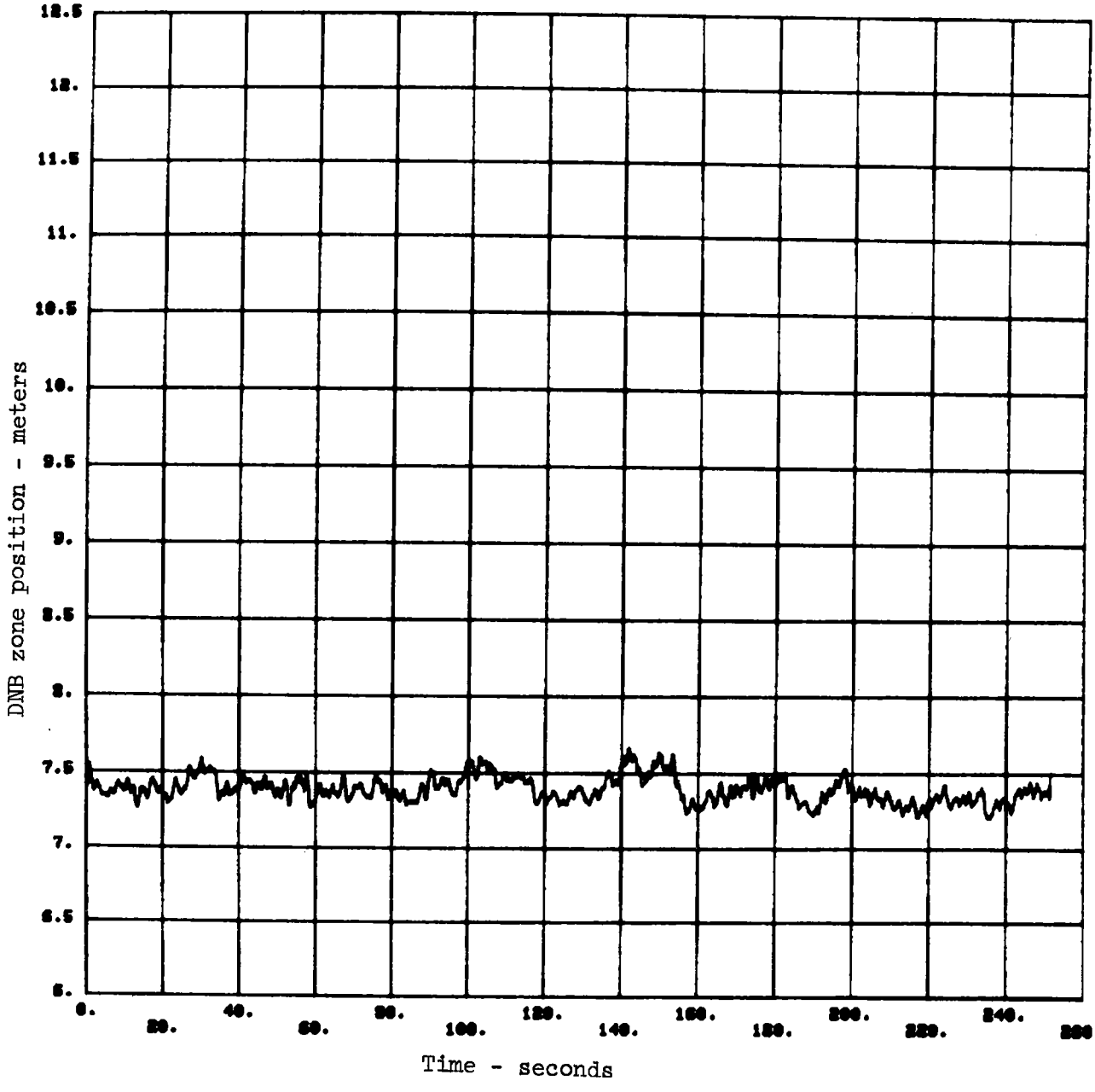

FIGURE 13
TEST POINT 5.4
13 JUNE 1979
ZERO SECONDS STARTS AT 14:41:47 HOURS

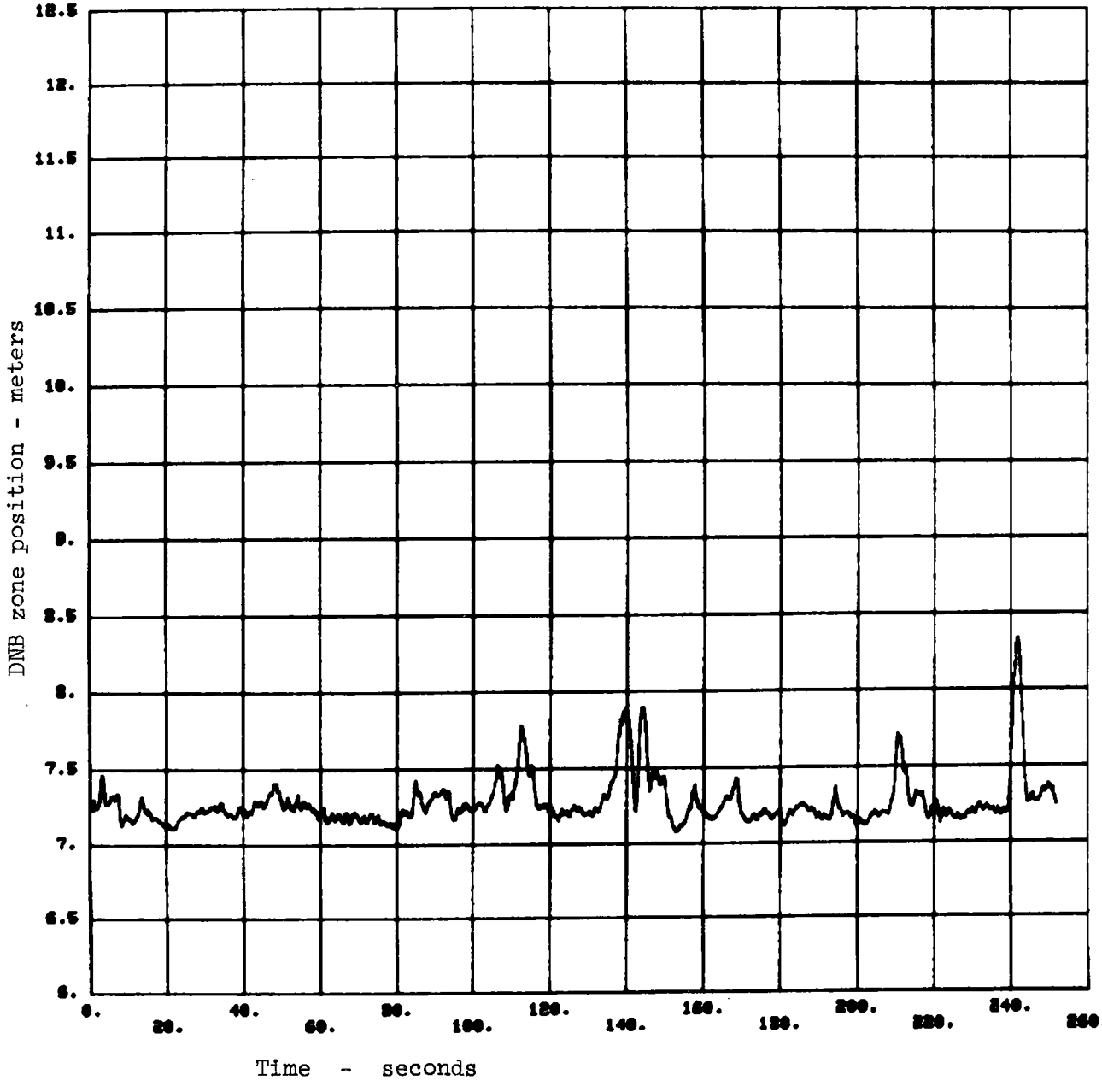

FIGURE 14
TEST POINT 5.5
13 JUNE 1979
ZERO SECONDS STARTS AT 15:13:09 HOURS

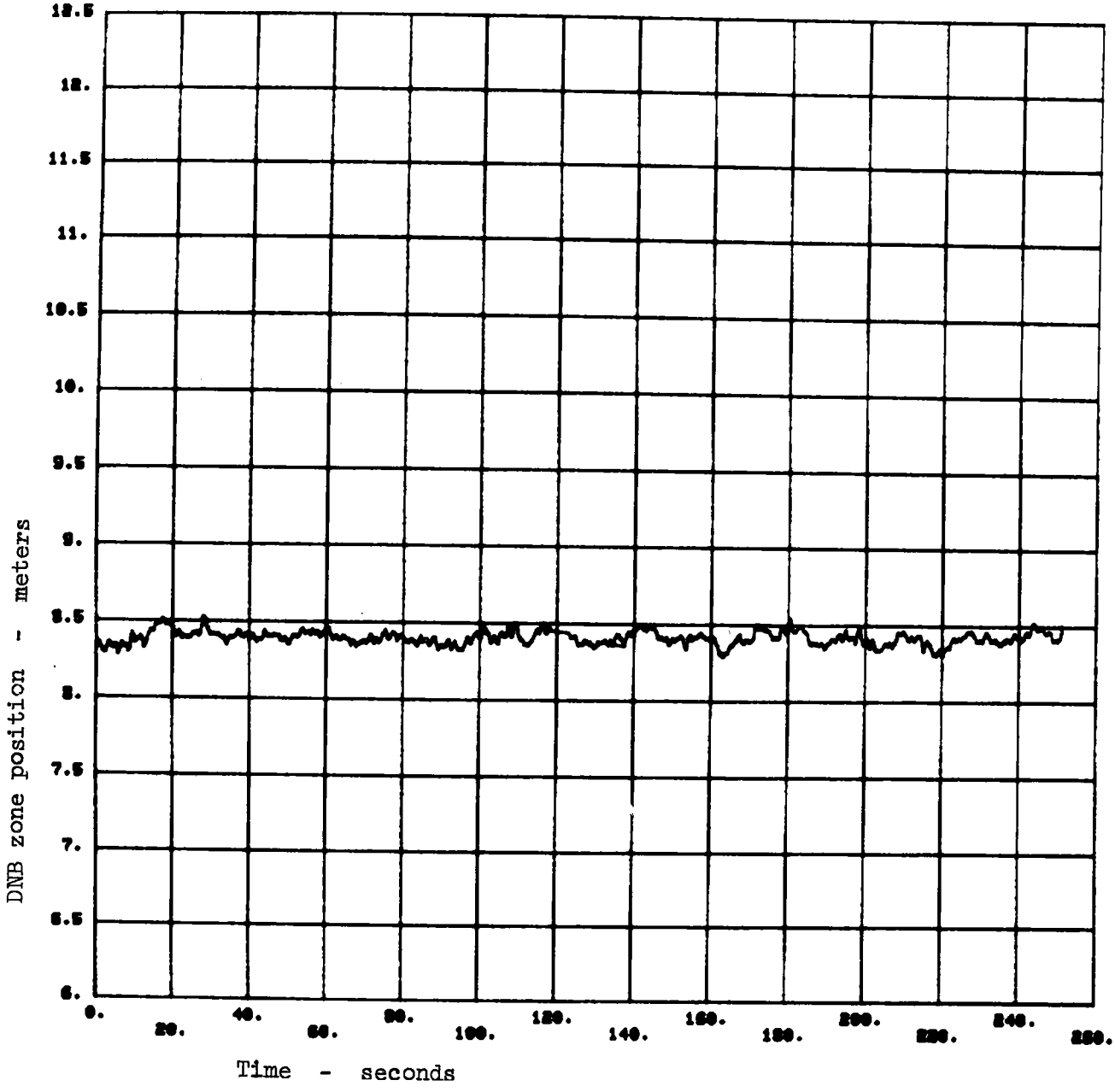

FIGURE 15
TEST POINT 5.6
13 JUNE 1979
ZERO SECONDS STARTS AT 15:45:47 HOURS

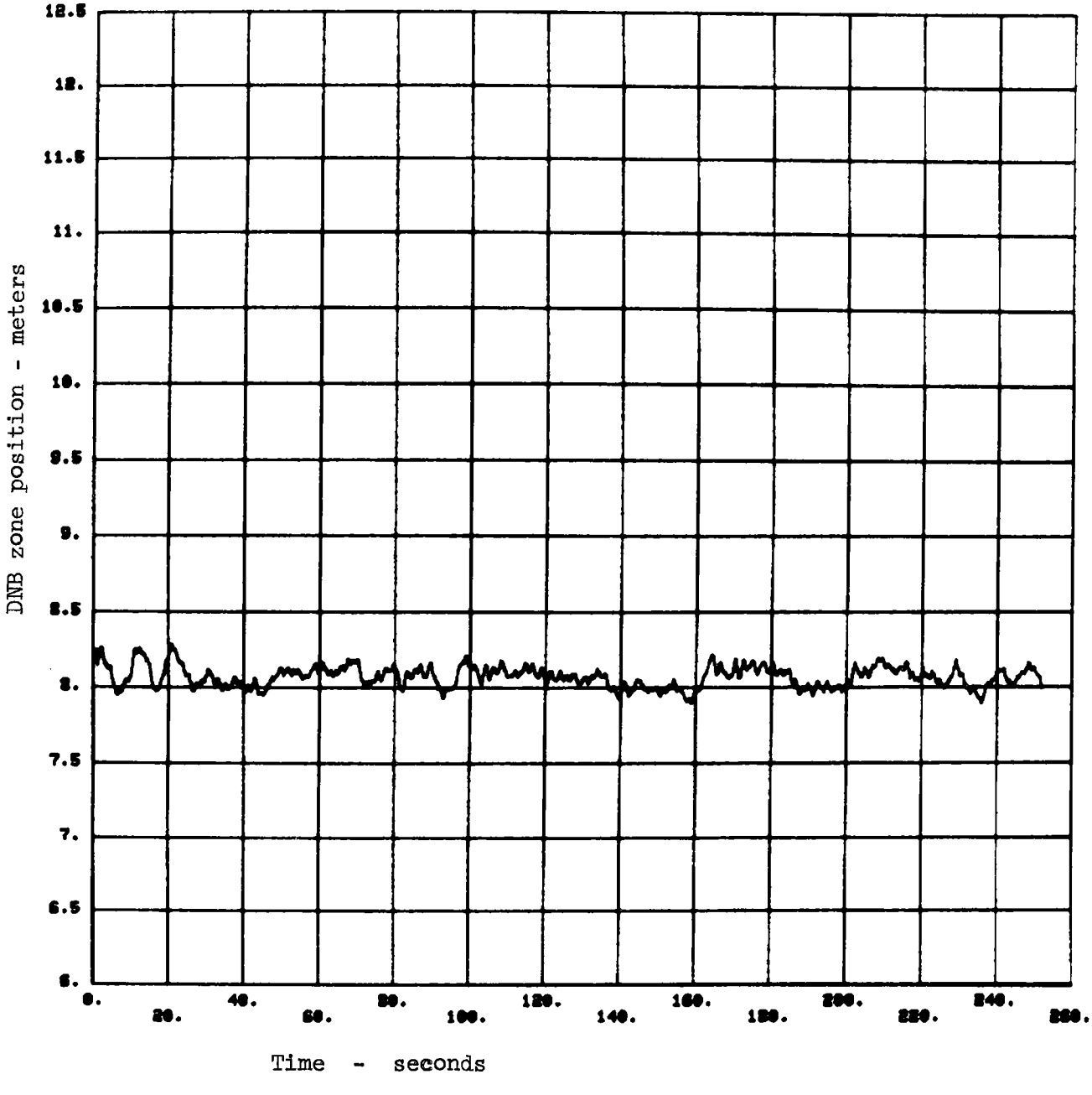

FIGURE 16
TEST POINT 21.8
13 JULY 1979
ZERO SECONDS STARTS AT 12:13:58 HOURS

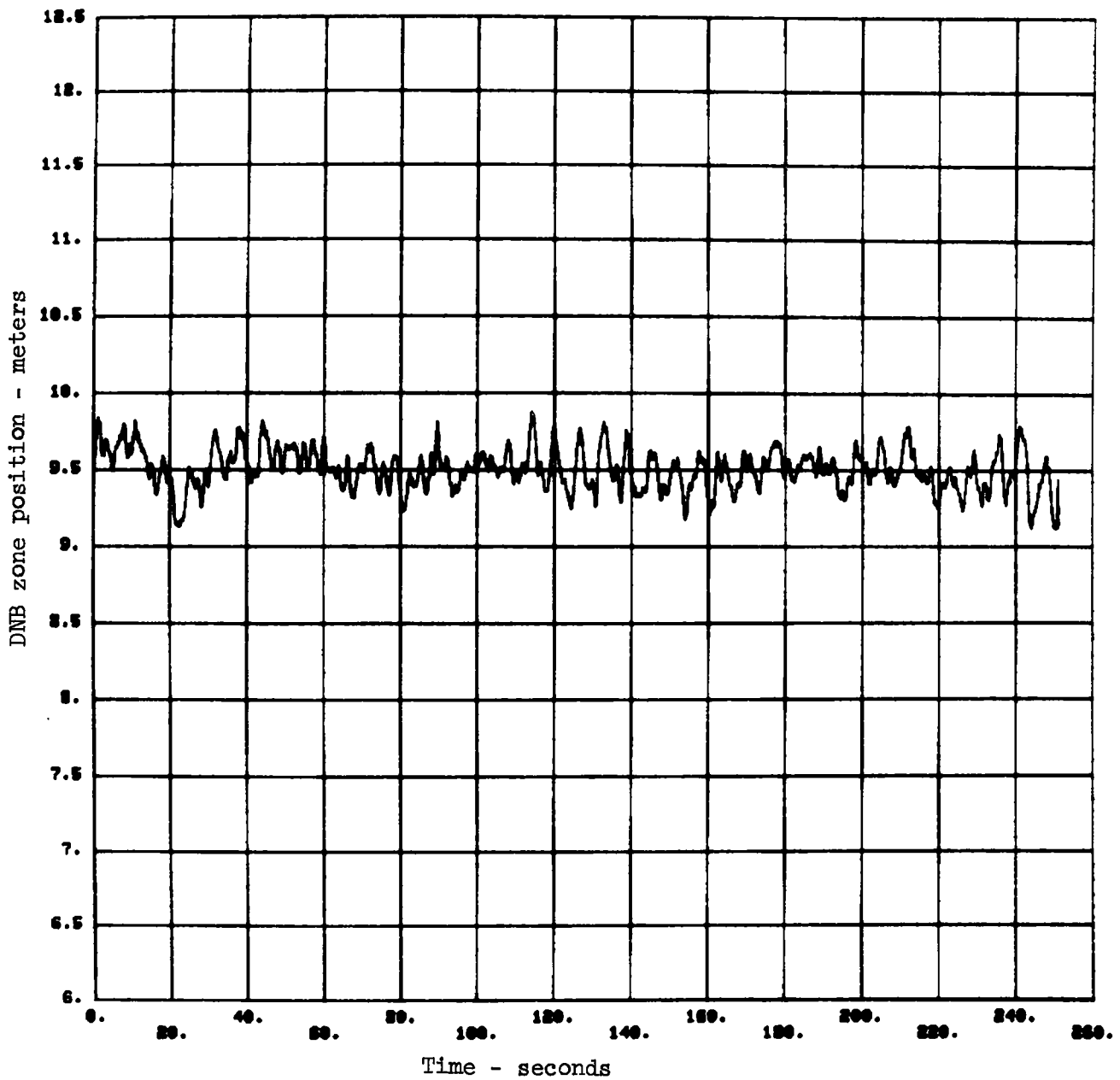

FIGURE 17
TEST POINT 21.9
13 JULY 1979
ZERO SECONDS STARTS AT 12:54:46 HOURS

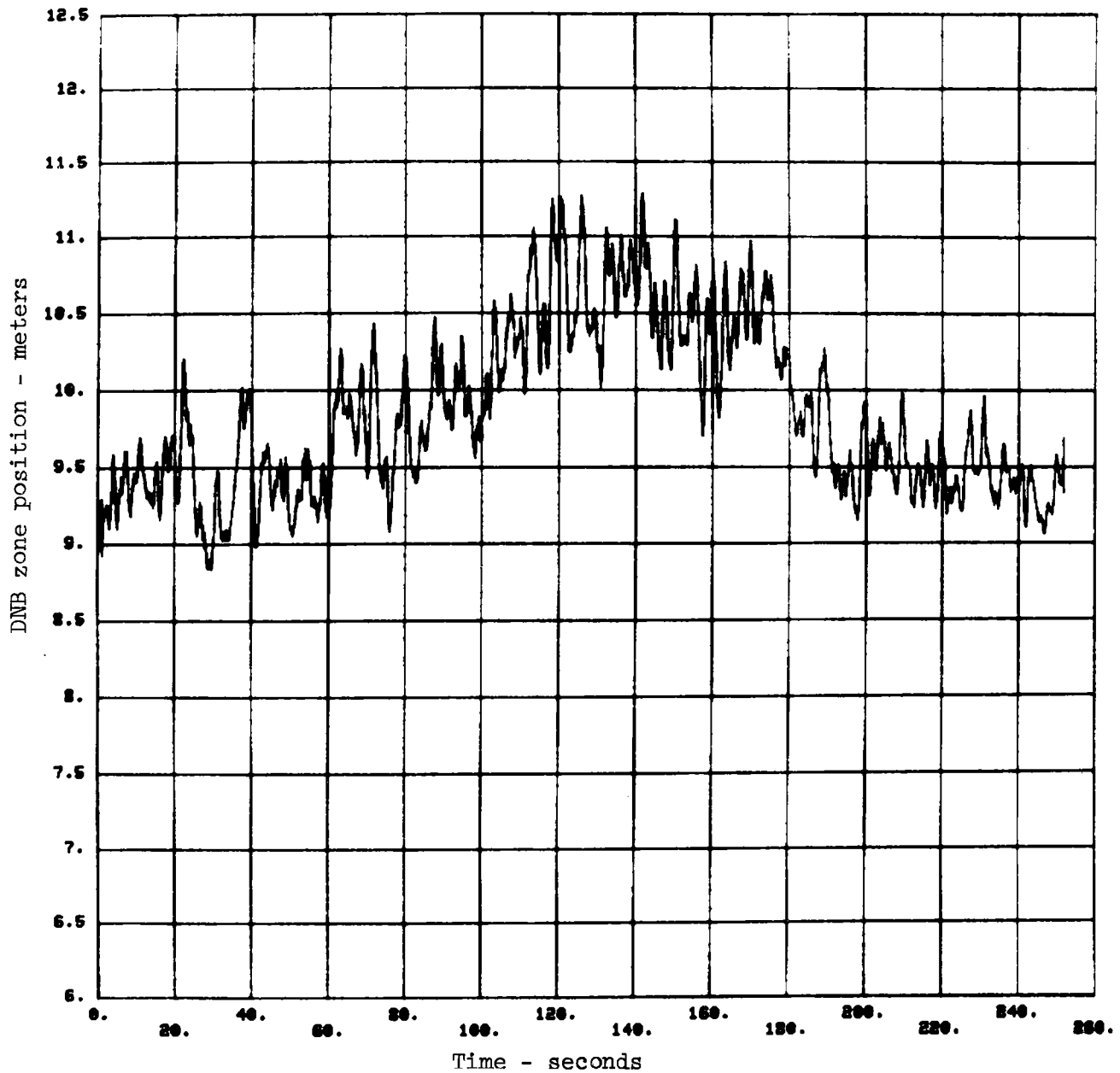

FIGURE 18
TEST POINT 21.10
13 JULY 1979
ZERO SECONDS STARTS AT 13:46:06 HOURS

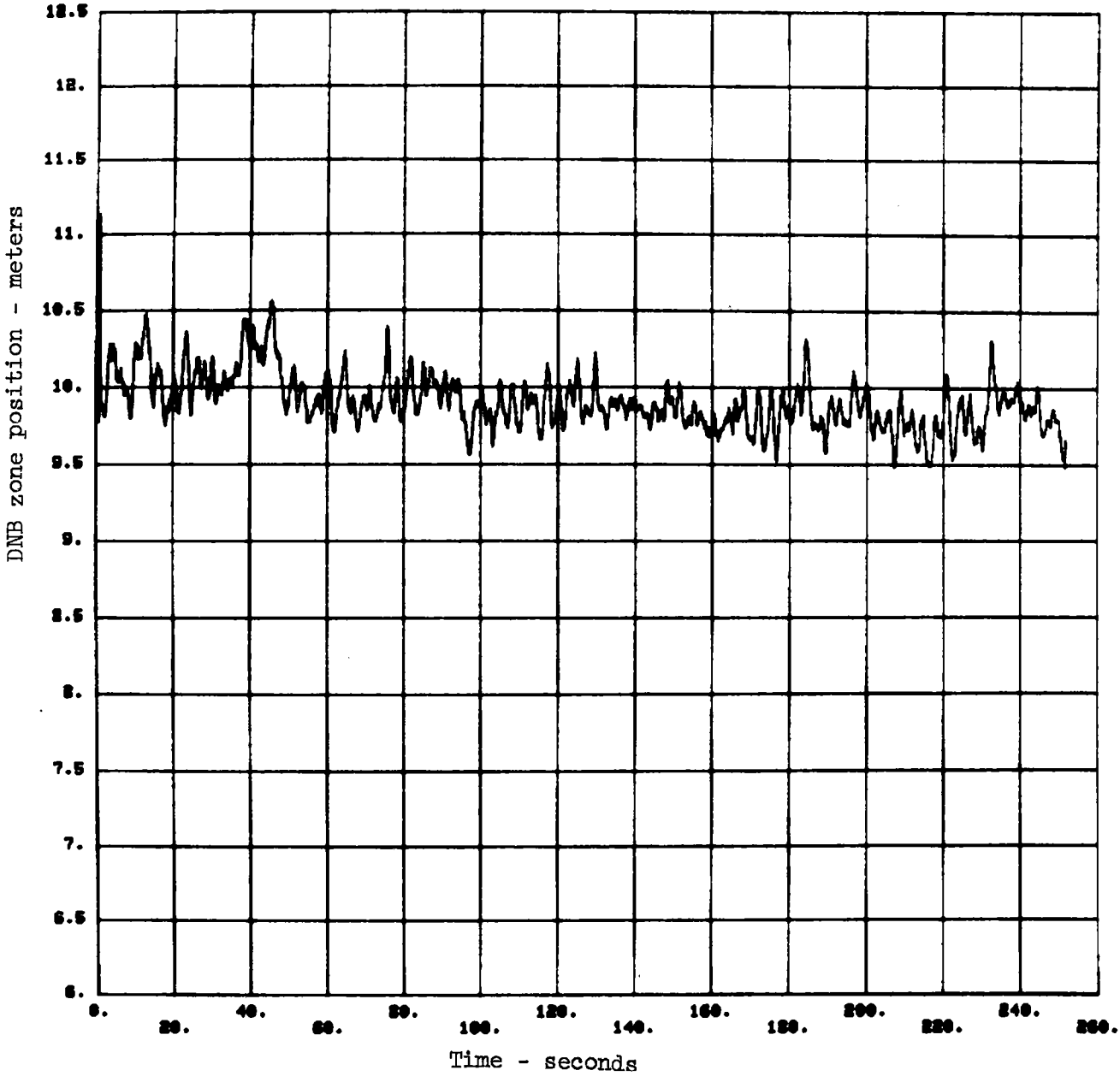

FIGURE 19
TEST POINT 21.11
13 JULY 1979
ZERO SECONDS STARTS AT 15:00:33 HOURS

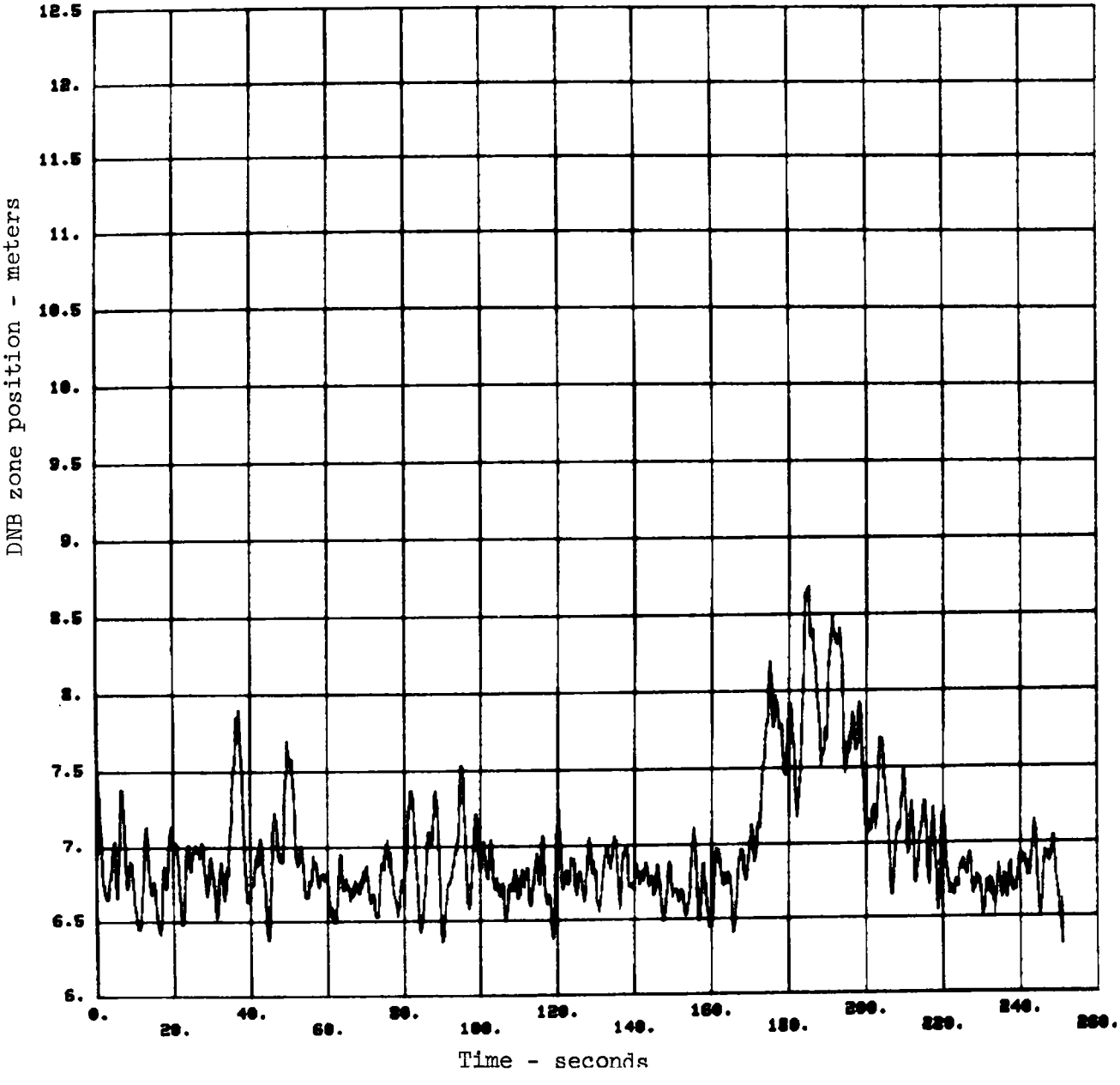

FIGURE 20
AN EXPANDED PLOT OF TEST POINT 21.09 SHOWING
THE OSCILLATIONS FROM 90 TO 180 SECONDS

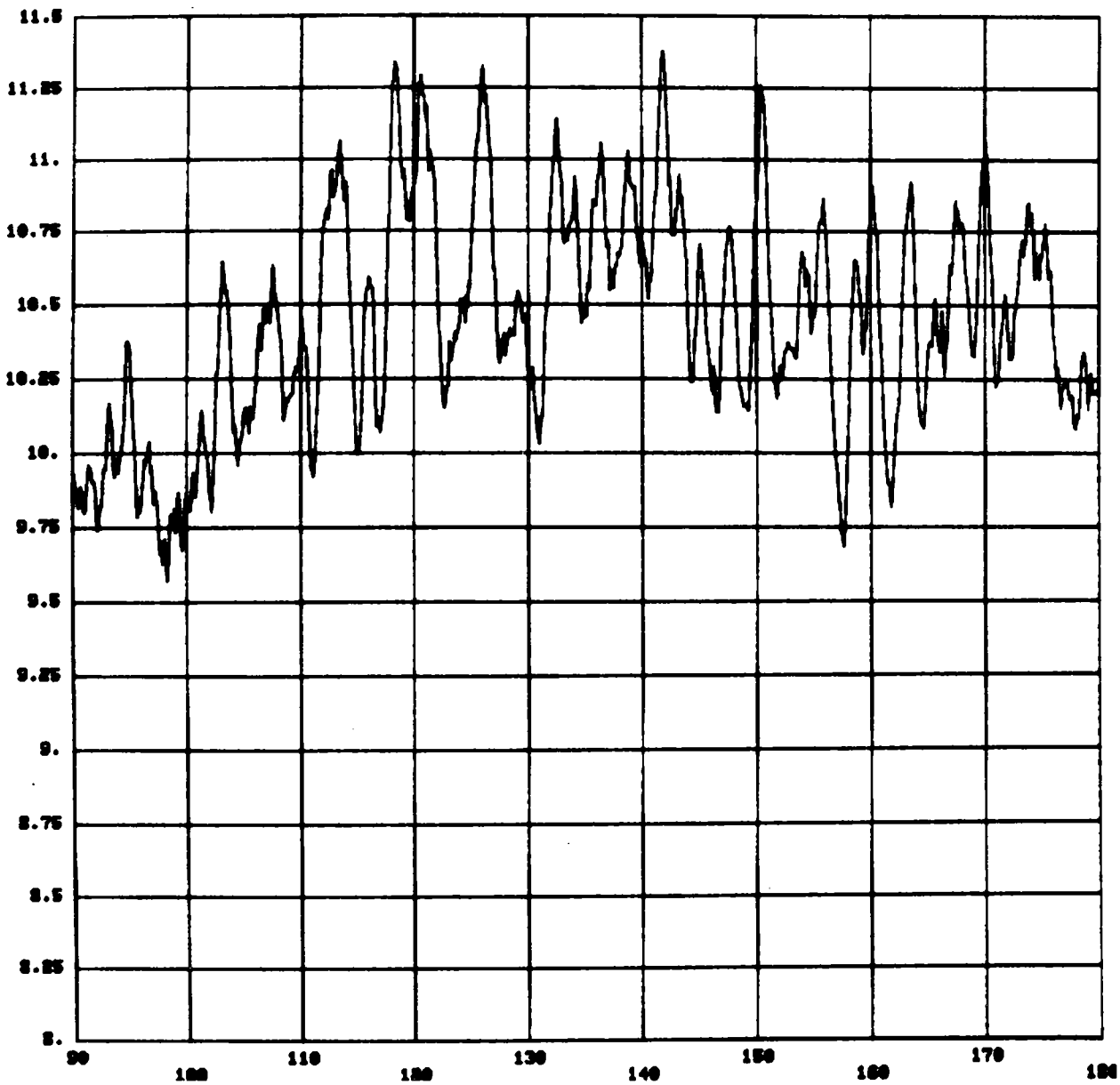

FIGURE 21
AN EXPANDED PLOT OF TEST POINT 21.09 USING THE AMPLITUDE FUNCTION SHOWN IN FIG. 2 IN THE ANALYSIS

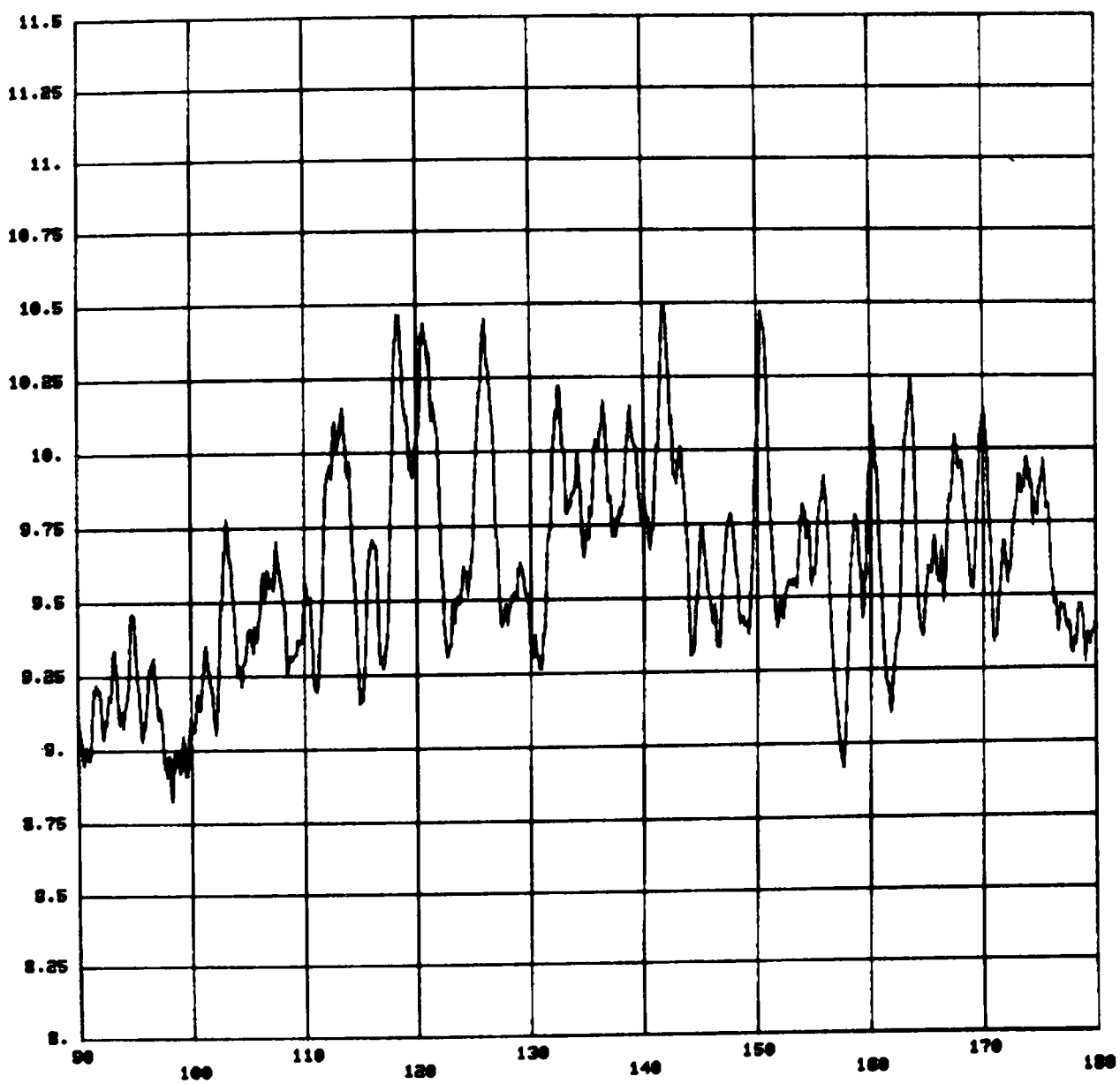

FIGURE 22
AN EXPANDED PLOT OF TEST POINT 21.09 USING THE SAME AMPLITUDE FUNCTION USED IN FIGURE 20 BUT USING ONLY THE DATA FROM THE CENTER 10 TRANSDUCERS IN THE ANALYSIS

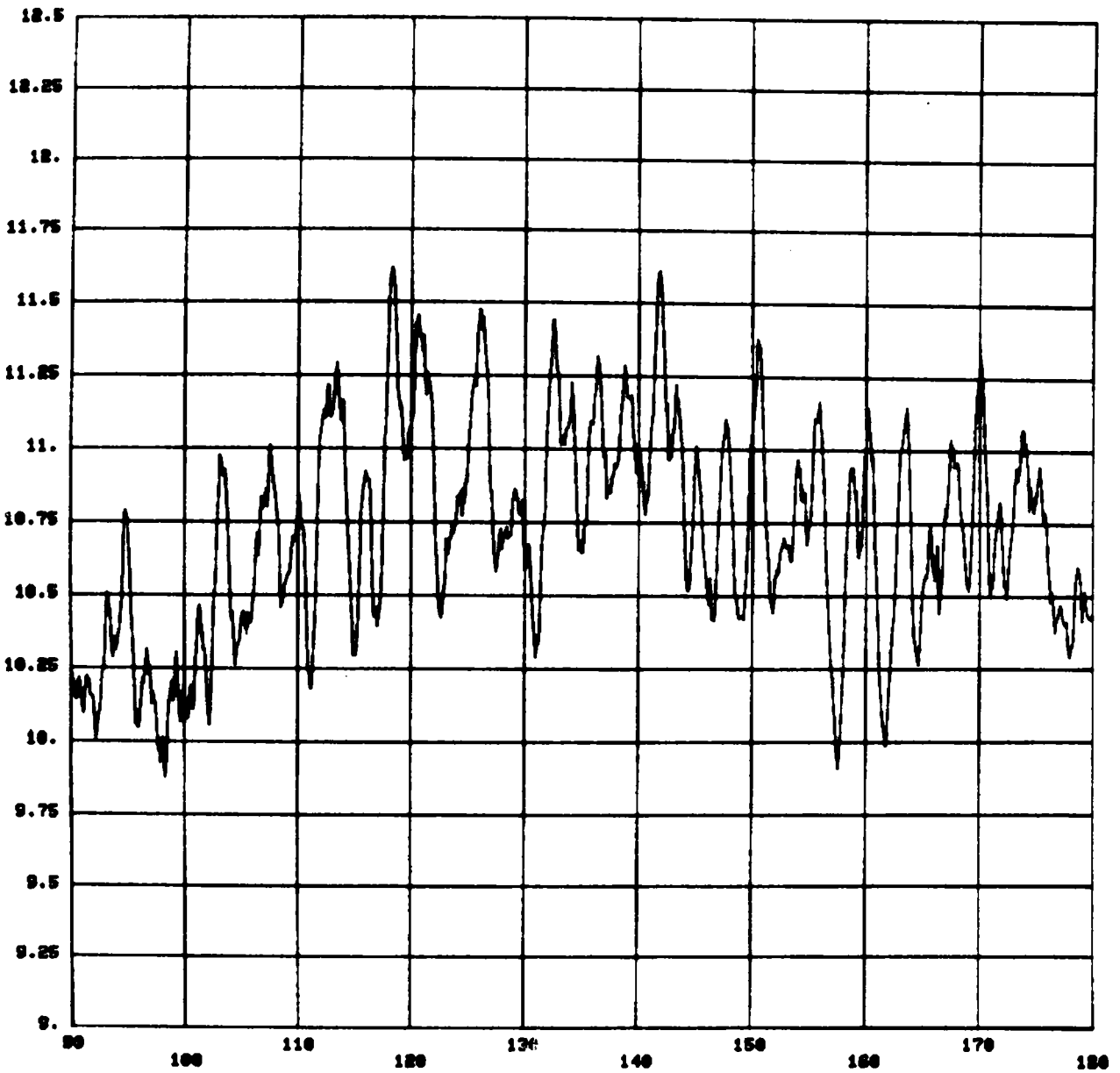

DISTRIBUTION:
Unlimited Release

J. Coleman
McDonnell Douglas Astronautics Company - West
5301 Bolsa Avenue
Huntington Beach, CA 92647

Rockwell Rocketdyne
6633 Canoga Avenue
Canoga Park, CA 91304
Attn: J. Friefeld, AB 48
R. Pauckert, AA 95
T. Neilson, AA 95
G. Batou, AC 34

1500 W. A. Gardner
1550 F. W. Neilson
1551 D. W. Ballard
1552 O. J. Burchett
1552 A. G. Beattie (20)
1552 J. A. Kinker
3141 T. L. Werner (5)
3151 W. L. Garner (3)
For: DOE/TIC
4700 J. H. Scott
4710 G. E. Brandvold
4713 B. W. Marshall
4713 L. O. Seamons
5510 D. B. Hayes
8444 A. R. Willis
8450 R. C. Wayne
8452 A. C. Skinrood
8452 E. T. Cull (10)
DOE/TIC (25)
(R. P. Campbell, 3154-3)

Org.	Bldg.	Name	Rec'd by *	Org.	Bldg.	Name	Rec

* Recipient must initial on classified documents.